The phonon density of states and high-resolution crystal structure of monoclinic tetracyanoethylene

1991 J. Phys.: Condens. Matter 3 9271

(http://iopscience.iop.org/0953-8984/3/47/002)

J. Phys.: Condens. Matter 3 (1991) 9271–9277. Printed in the UK

The phonon density of states and high-resolution crystal structure of monoclinic tetracyanoethylene

S L Chaplot†, R Chakravarthy†, W I F David‡ and J Tomkinson‡

† Solid State Physics Division, Bhabha Atomic Research Centre, Bombay 400 085, India

‡ Neutron Science Division, Rutherford Appleton Laboratory, Chilton, Didcot, Oxon OX11 0QX, UK

Received 24 April 1991

Abstract. The phonon density of states in the monoclinic phase of tetracyanoethylene is investigated at 20 K using inelastic neutron scattering, and found to be in fair agreement with theoretical calculations based on a semi-rigid molecule model and 6-exponential pair potentials. The results provide support for the atom–atom potential model which was used to explain the relative stability of different phases in this solid. The monoclinic crystal structure at 295 K is also refined using powder neutron diffraction data with a higher resolution than in earlier reports. Comparison is made with the molecular geometry in the cubic phase.

1. Introduction

Considerable interest exists in the study of interatomic interactions in complex solids through investigations of lattice dynamics, structures and phase transitions. (See [1] and [2–4] for earlier references on ionic and organic solids respectively.) Amongst organic solids, tetracyanoethylene (TCNE, $C_2(CN)_4$, ethylenetetracarbonitrite) has been of special interest for a variety of reasons. It is a simple system with only two types of atoms, namely C and N, and forms a number of electron donor–acceptor complexes leading to special properties. Further, TCNE has peculiar phase transitions involving crystalline and amorphous phases [4–7]. TCNE is also one of the simplest materials having a strong coupling of the intramolecular and intermolecular vibrations [8–10] leading to complex phonon spectrum and distortion of the molecular geometry in various solid phases.

At atmospheric pressure, the cubic phase I of TCNE transforms to the monoclinic phase II on heating at 318 K [7], and the transformation is irreversible on cooling to 5 K [8]. However, on application of a pressure of 2 GPa at 295 K, the reverse transition from phase II to I is observed via an intermediate metastable amorphous phase III [5]. A detailed study of the phonon dispersion relation in the monoclinic phase of TCNE along high symmetry directions has been carried out by coherent inelastic neutron scattering [8], while the zone centre phonons have been studied extensively in both phases I and II by Raman scattering [9] as a function of pressure. These experimental studies have been comprehensively supported by lattice dynamical calculations [4, 8–10] of thermal vibrations. The calculations are based on the 6-exponential atom–atom pair potential [11] between non-bonded atoms and the semi-rigid molecular model [8]. The crystal

0953-8984/91/479271+07$03.50

structures of both phase I [12, 13] and II [14, 15] have been studied by neutron and x-ray diffraction. For completeness, we note that studies of Brillouin scattering [16] and electrical resistivity [17] have also been carried out.

As the results of the earlier lattice dynamical calculations agreed very well with experiments, we have calculated and compared the Gibbs free energies for the two crystalline phases I and II of TCNE as a function of temperature and pressure, in order to understand the phase diagram [4]. The lattice part of the free energy has contributions from the molecular packing and the phonon density of states. While the two phases are found to have almost equal static potential energy, it is shown [4] that the low-symmetry monoclinic phase is stabilized at high temperature due to its higher vibrational entropy, as compared to the cubic phase which is stabilized at high pressure due to its lower volume. It is particularly noteworthy that the calculated differences in the phonon spectra of the two phases, among other factors, are found to have a subtle relationship with the relative stability of those phases as a function of temperature [4].

In order to test the validity of the calculated phonon density of states, we have now performed inelastic neutron scattering experiment on a powder sample of the monoclinic phase. Such a measurement provides the phonon spectrum integrated over the entire Brillouin zone, whereas the earlier experiment [8] using a single crystal provided details of the phonon dispersion relation along the measured directions of the wave vector only. The measurements reported in this paper have been carried out at the spallation pulsed neutron source of the Rutherford Appleton Laboratory (RAL, UK). These results are consistent with later measurements [18] carried out with a somewhat poorer energy resolution as a part of feasibility studies for such work at the Dhruva reactor (India). Apart from the results on the phonon spectrum, in this paper we also report a new refinement of the crystal structure of the monoclinic phase using high-resolution data from a powder neutron diffraction experiment also carried out at RAL.

2. Experiment

Commercial TCNE was purified by sublimation and recrystallized from solution in ethyl acetate by slow evaporation at 300 K to obtain the sample in monoclinic phase. The procedure is described in detail elsewhere [7].

The inelastic neutron scattering experiment was carried out on the neutron spectrometer TFXA (Time Focussed Crystal Analyser) at RAL. The neutron time-of-flight data were collected for a fixed scattering angle of 133° and a fixed value of the scattered neutron energy of 4.0 meV using a pyrolytic graphite analyser. The energy resolution was $\Delta E/E \leqslant 2.5\%$ for the energy transfer E between 2 to 180 meV [19]. The data were collected with a total of 500 μA h of the incident neutron beam on 15 g of the sample held at 20 K at ambient pressure.

The neutron diffraction data were obtained using the high-resolution powder diffractometer (HRPD) at RAL under ambient temperature and pressure. For the back-scattering geometry of the detector bank, this instrument provides a very good resolution of $\Delta d/d = 4 \times 10^{-4}$, which is much better than that of usual powder diffractometers.

3. Phonon density of states

3.1. Data analysis

The time-of-flight data were analysed, with suitable subtraction of the background intensity and using the standard procedure at RAL [19], to obtain the neutron-weighted dynamical structure factor $S(\boldsymbol{Q}, E)$. Here $\boldsymbol{Q}$ and E denote the wave vector and energy transfer respectively. The measurement on the powder sample produces directional averaging of $\boldsymbol{Q}$. From $S(Q, E)$ one obtains the neutron-weighted density of states $g^{(n)}(E)$ using equation (1) given below.

For the neutron energy loss experiment, we have

$$g^{(n)}(E) = S(Q, E)\frac{E e^{Q^2u^2/3}}{Q^2[n(E,T)+1]} \tag{1}$$

$$n(E,T) = \frac{1}{e^{(E/KT)}-1} \tag{2}$$

$$g^{(n)}(E) = \sum_k g_k(E) b_k^2/m_k \tag{3}$$

$$g(E) = \sum_k g_k(E)\,. \tag{4}$$

Here the mean-squared atomic displacement u^2 is assumed to be the same for both C and N atoms as it is very small at the low temperature of $T = 20$ K. The partial contributions $g_k(E)$ from the different atomic species (C and N) are weighted by their respective 'neutron scattering weightage factors' b_k^2/m_k (b_k = scattering length and m_k = mass of the atom k) to yield $g^{(n)}(E)$, whereas the true density of states $g(E)$ is merely the sum of the partial density of states from each atom. Equation (1) is strictly true only in the 'incoherent approximation', in which it is assumed that, when the scattered intensity is summed over a large number of phonon wave vectors $\boldsymbol{q}$, the correlation between the atomic motions may be ignored. This is, however, true only for a sufficiently large value of $\boldsymbol{Q}$ to allow averaging over several reciprocal lattice vectors $\boldsymbol{G}(= \boldsymbol{Q} \pm \boldsymbol{q})$. In our experiment $\boldsymbol{Q}$ varied from 26 nm^{-1} to 54 nm^{-1} for the energy transfer E from 0 to 36 meV respectively, while the smallest $\boldsymbol{G}$ is 12 nm^{-1}. Therefore the $g^{(n)}(E)$ as obtained from this experiment would involve a better $\boldsymbol{Q}$-averaging at higher energies as compared to that at lower energies. However the peak positions in $g^{(n)}(E)$ may not be much affected but only the peak heights. Figure 1 gives the plot of $g^{(n)}(E)$, for E up to 36 meV which is expected [4] to cover the range of external vibrations and the low energy internal vibrations.

3.2. Comparison with theoretical calculation

The phonon density of states in TCNE was calculated [4] using the semi-rigid molecular model, which includes the contributions from all the intermolecular vibrations and those of the intramolecular vibrations relevant in the energy region of 0 to 36 meV. Figure 2 gives the calculated total one-phonon neutron-weighted density of states $g^{(n)}(E)$, which is obtained by suitable weighted summation over the partial phonon density of states [4]. The multi-phonon contribution is separately obtained for the temperature of 20 K and the experimental values of $\boldsymbol{Q}$, using Sjolander's formalism [20]. This multi-phonon part, however, turns out to be below 1.5% of the maximum in $g(E)$ and is therefore neglected in comparison of overall errors and approximations.

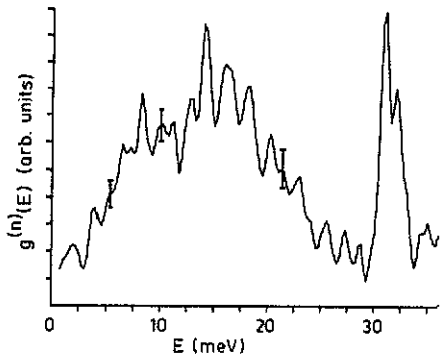

Figure 1. The observed neutron-weighted phonon density of states in the monoclinic phase of TCNE at 20 K.

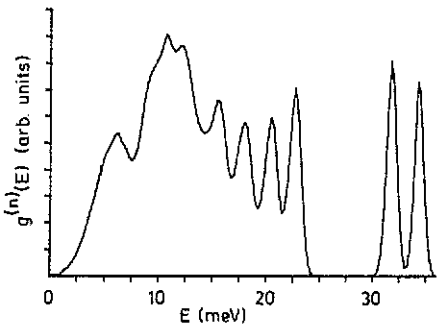

Figure 2. The calculated neutron-weighted phonon density of states in the monoclinic phase of TCNE.

The experimental results in figure 1 are in good agreement with the calculations in figure 2 in terms of the overall shape, and the band gap at 25 to 30 meV. The results thus provide the essential support for the lattice dynamical model of TCNE and its use in understanding the phase transitions [4].

4. Crystal structure

The powder diffraction pattern is given in figure 3. The structure refinement is carried out using the available data analysis program VDELSQ at RAL [21] employing the Rietveld technique. The refinement included data in the d-spacing range of 0.083 to 0.27 nm. The lower limit is smaller than the minimum d-value included in the earlier work [15] (0.125 nm at 295 K and 0.097 nm at 5 K). The present work also involves improvement in resolving the diffraction peaks at small d-spacing ($\Delta d/d = 4 \times 10^{-4}$, compared to 10^{-3} in [15]). For these reasons it is now also possible to refine from the powder data the anisotropic temperature factors at 295 K for all the atoms with physically meaningful values. The result of the refinement of the crystal structure is given in table 1. The statistical errors obtained from the refinement program tend to be rather low since the number of observed data points is quite large. In table 1 we

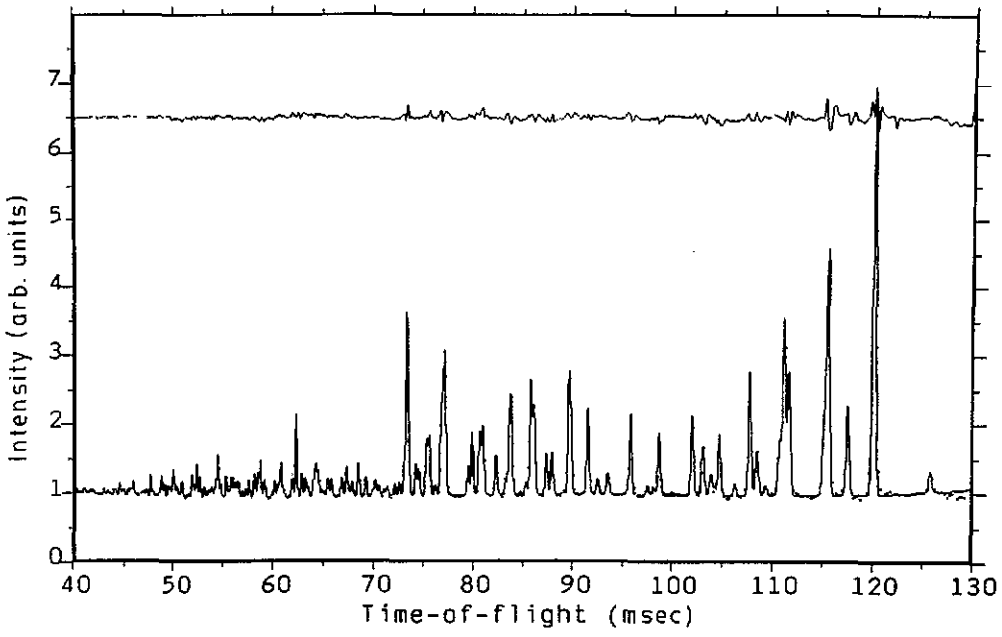

Figure 3. The powder neutron diffraction pattern at 295 K from the monoclinic phase of TCNE. The points give the observed data and full line gives the calculated plot from the refined structure. The difference plot is also given. The d-spacing = time of flight $\times 2.07$ nm s^{-1}.

Table 1. Results of the structure refinement of the monoclinic TCNE at 295 K. Space group $P2_1/n$, 2 formula units per cell, $a = 0.74890(2)$ nm, $b = 0.62045(2)$ nm, $c = 0.69911(2)$ nm, $\beta = 97.235(1)^\circ$, $V = 0.32225$ nm^3, profile R-factor = 0.030, intensity–intensity R-factor = 0.075, weighted profile R-factor = 0.0347 and its expected value = 0.0182. For definitions see [21].

Atom position	C(1)	C(2)	C(3)	N(2)	N(3)
	Fractional Coordinates (ESD[a] = 0.0003)				
X	0.0023	0.0837	−0.0757	0.1497	−0.1381
Y	−0.0382	0.0821	−0.2438	0.1788	−0.4055
Z	−0.0881	−0.2251	−0.1465	−0.3410	−0.1942
	Thermal parameters[b] (ESD[a] = 0.1)				
B_{11}	2.74	3.52	3.22	6.14	5.41
B_{22}	4.53	4.06	4.39	5.76	4.05
B_{33}	3.89	6.57	5.06	6.57	6.92
B_{23}	0.86	0.18	0.40	1.01	−0.48
B_{13}	−0.04	0.06	−0.45	2.59	−0.86
B_{12}	0.15	0.47	0.21	−0.53	−1.15

[a] ESD means estimated standard deviation.
[b] The thermal parameters B_{ij} are given in Å^2. The expression used for temperature factor is $\exp[-0.25(B_{11}ha^*ha^* + \cdots + 2B_{23}kb^*lc^* + \cdots)]$.

have quoted a realistic error estimate based on the variation in the results obtained from slightly different refinements involving different ranges of d-spacings.

Table 2 gives a comparison of the structure data with earlier work which shows a fair agreement. The present values of the structure data at 295 K may be considered more accurate than the earlier work since these have been refined from a better resolution experiment. We wish to draw attention to the central C=C double bond length. The present result of 0.1328 (5) nm is close to the value of 0.1317 (9) nm as obtained from the x-ray work [14]. This bond length in the monoclinic structure seems to be really smaller than the value of 0.1353(3) nm in the cubic structure [12]. The other bond lengths in the cubic phase [12] are 0.1432(2) and 0.1166(2) nm for the C—C and C=N bonds respectively, which are comparable to the values in the monoclinic phase.

Table 2. Comparison of present crystal structure results with earlier results from neutron and x-ray diffraction.

	Present work	Earlier work	
	Neutron powder	Neutron powder [15]	x-ray single crystal [14]
Unit cell constants at 295 K			
a (nm)	0.74890 (2)	0.7501 (2)	0.751 (1)
b (nm)	0.62045 (2)	0.6218 (5)	0.621 (1)
c (nm)	0.69911 (2)	0.7004 (6)	0.700 (1)
β (°)	97.235 (1)	97.22 (5)	97.17 (10)
Bond lengths[a] (nm)			
Central C=C	0.1328 (5)	0.1370 (24)	0.1317 (9)
Average C−C	0.1431 (5)	0.1425 (9)	0.1449 (4)
Average C≡N	0.1156 (5)	0.1150 (9)	0.1132 (5)

[a]Libration corrections from rigid-body approximation [14] are included. The corrections at 295 K added to the three bond lengths are 0.0004, 0.0005 and 0.0003 nm respectively.

5. Summary

This paper presents new results on the crystal structure and molecular dynamics in tetracyanoethylene which form important input to the complete study of the interesting phase transitions in this organic material. In particular the inelastic neutron scattering results provide support for the atom–atom potential model which is used [4] to understand the relative stability of the different phases in TCNE.

Acknowledgments

SLC and RC wish to thank K R Rao for his kind encouragement and support, and S K Paranjpe for part of the structure refinement. SLC also thanks R Mukhopadhyay for collaboration in related earlier work.

References

[1] Rao K R and Chaplot S L 1985 *Phonon Physics* ed J Kollar, N Kroo, N Menyhard and T Siklos (Singapore: World Scientific) pp 175–178
Chaplot S L 1988 *Phys. Rev.* B **37** 7435; 1990 *Phys. Rev.* B **42** 2149
[2] Pawley G S 1986 *Methods of Experimental Physics* vol 23A (New York: Academic) p 441
[3] Dove M T, Powell B M, Pawley G S, Chaplot S L and Mierzejewski A 1989 *J. Chem. Phys.* **90** 1918
[4] Chaplot S L 1987 *Phys. Rev.* B **36** 8471
[5] Chaplot S L and Mukhopadhyay R 1986 *Phys. Rev.* B **33** 5099
[6] Chaplot S L 1985 *Phys. Status Solidi* a **92** K 23
[7] Mukhopadhyay R, Chaplot S L and Rao K R 1985 *Phys. Status Solidi* a **92** 467
[8] Chaplot S L, Mierzejewski A, Pawley G S, Lefebvre J and Luty T 1983 *J. Phys. C: Solid State Phys.* **16** 625
[9] Chaplot S L, Mierzejewski A and Pawley G S 1985 *Mol. Phys.* **56** 115
[10] Chaplot S L 1985 *J. Phys. C: Solid State Phys.* **18** 2055
[11] Govers H A J 1975 *Acta Crystallogr.* A **31** 380
[12] Little R G, Paulter D and Coppens P 1971 *Acta Crystallogr.* B **27** 1493
[13] Becker P, Coppens P and Ross F K 1973 *J. Am. Chem. Soc.* **95** 7604
[14] Bekoe D A and Trueblood K N 1960 *Z. Kristallogr.* **113** 1
[15] Chaplot S L, Mierzejewski A and Pawley G S 1984 *Acta Crystallogr. C* **40** 663
[16] Mierzejewski A and Ecolivet C 1982 *J. Phys. C: Solid State Phys.* **15** 4695
[17] Sahu P C, Govinda Rajan K, Yousuf M, Mukhopadhyay R, Chaplot S L and Rao K R 1989 *Pramana (J. Phys.)* **33** 667
[18] Chaplot S L, Mukhopadhyay R, Vijayaraghavan P R, Deshpande A S and Rao K R 1989 *Pramana (J. Phys.)* **33** 595
[19] Penfold J and Tomkinson J 1986 *Rutherford Appleton Laboratory Report* RAL-86-019
[20] Sjolander A 1958 *Ark. Fys.* **14** 315
[21] David W I F, Akporiaye D E, Ibberson R M and Wilson C C 1988 *Rutherford Appleton Laboratory Report* RAL-88-103